



## Effect of arch height on wind load in shape dome structure

Saeid Khosrowjerdi<sup>1</sup>, Hamed Sarkardeh<sup>1,\*</sup>

Department of Civil Engineering, Faculty of Engineering, Hakim Sabzevari University, Sabzevar, Iran

**ABSTRACT:** In an optimal design of a dome building, the outer shell with a curved shape, plays an important role in the architectural approach, bearing capacity, and the structural strength in vertical and lateral loads. In this research, the effect of the arch in domes against the wind is studied, numerically. For this purpose, domes with fixed height–diameter proportion in Type C ground and with the speed and turbulence intensity matching ASCE7 regulations are numerically simulated and the amounts of pressure coefficients ( $C_p$ ) are represented on the central line corresponding to the wind direction and the rings around the dome with different heights including 0, 0.25h, 0.5h, 0.75h, and h. Results indicated the great effect of arch height on  $C_p$  and the percent of under pressure surfaces.

**Review History:**

Received: 5/26/2019

Revised: 1/16/2020

Accepted: 2/3/2020

Available Online: 3/10/2020

**Keywords:**

DOME

CFD

WIND LOAD

SPATIAL STRUCTURE

ARCH

**1. INTRODUCTION**

In the geometry design of domes, a number of factors along with the lateral loads exerted are usually taken into account. Some research studies have shown that, specifically, domes to be resistant to symmetrical loads while they are susceptible to asymmetrical loadings like those created by wind or snow [1]. Also, the load created by wind is a function of the structure geometry. The present study is an attempt to investigate the effect of height in the arch of domes on the experienced wind load. For this purpose, five different arches of domes with different heights and similar height–diameter proportions are studied against the wind (Fig. 1a).

**2. MATERIALS AND METHODS**

The present research investigates the effect of the form of domes on  $C_p$ , which is a non-dimensional parameter and can be obtained by  $c_p = \frac{\Delta P}{0.5\rho U^2}$ , where,  $\rho$  and  $U$  are the density of air and its velocity, respectively.  $\Delta P$  is the pressure difference between the dome surface pressure  $P$  and free-stream pressure  $P_1$ . The prototype dome dimensions, which are selected for this study, have an approximate sphere diameter of 168m. The sphere diameter was truncated to a base diameter of 144m and a height of 45m. Letchford and Sarkar [2] studied models of parabolic domes of nearly spherical shape, with a base diameter of 480mm and an apex height of 150mm (Fig. 1b). The wind tunnel created a

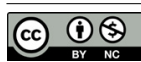
simulation of Exposure C, ASCE7-98 wind code conditions at a scale of 1:300 by using 4 upwind spires, a 240mm fence, and 18mm chain floor roughness at 200mm spacing up to the model domes. The mean velocity and turbulence intensity at model apex height are 18m/s and 15%, respectively. *Reynolds* is approximate,  $4.6 \times 10^5$ . Boundary layer characteristics are also the target values for inlet conditions to the test domain for numerical calculations.

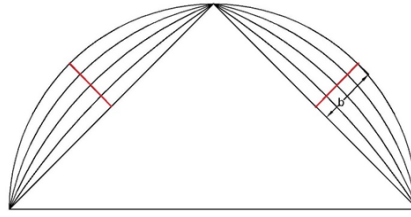
**3. NUMERICAL PROCEDURE**

This paper evaluates the  $C_p$  on the surface of the dome based on 3D steady RANS-RNG implementing Ansys-Fluent software. Fig. 2 presents the numerical inlet velocity and turbulent intensity profiles compared to the wind-tunnel measurements and target ASCE7-98 Exposure C code profiles. The profile of Figs. 2(a) and 2(b) are used to apply the average imposed velocity to the software and the intensity of turbulence concordant to the ground, respectively. It is not possible to directly apply the profile of turbulence intensity to the Ansys-Fluent software; therefore, values are applied through turbulent kinetic energy ( $k$ ) and turbulent dissipation rate ( $\varepsilon$ ). As it is shown in Fig. 2, applied profiles are by the experimental models.

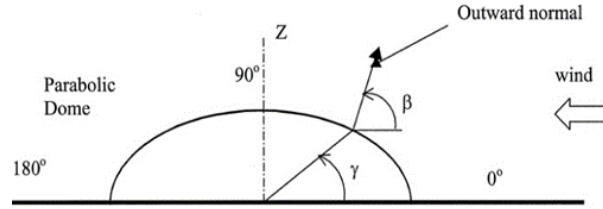
$$K = \frac{3}{2}(U_{avg} I)^2 \quad (1)$$

\*Corresponding author's email: sarkardeh@hsu.ac.ir



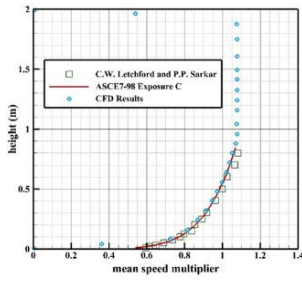


(a) Dome with height – diameter proportion of 0.5 with arch heights of 0, 0.25b, 0.5b, 0.75b and b

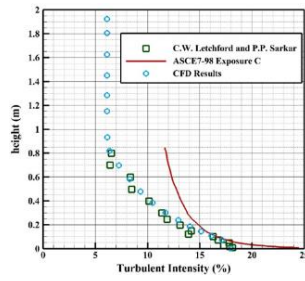


(b) Parabolic dome of Letchford and Sarkar [2]

Fig. 1. Schematic view of the simulated geometries



(a) velocity profile



(b) Turbulent intensity profile

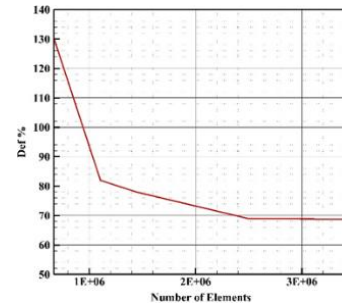
Fig. 2. Different numerical inlet profile compared to the wind-tunnel measurements and target ASCE7-98 Exposure C code profiles

$$\varepsilon = \frac{K^{\frac{3}{2}}}{l} \quad (2)$$

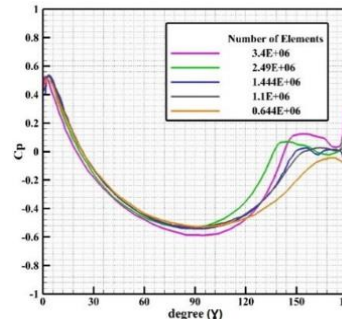
$$l = \frac{0.07L}{C_{\mu}^{\frac{3}{4}}} \quad (3)$$

where,  $U_{avg}$  is the average ratio of speed to velocity,  $I$  is the intensity of turbulence,  $l$  is the hydraulic diameter, and  $C_{\mu}$  is the coefficient of the ground type.

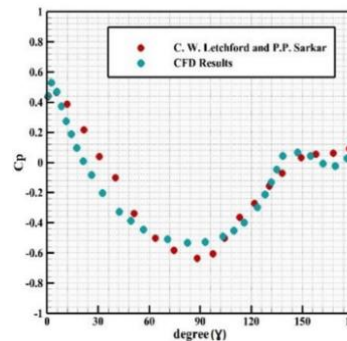
Results of numerical analysis are shown for  $\beta$  angle in the range of 0 to 180 degrees, calculated along the meridian in the wind direction. Fig. 3(a) and (b) evaluates the effect of size and number of the mesh over the accuracy of the CFD results. As it is clear from Fig. 3(b) the number of  $2.49 \times 10^6$  mesh has the most accordance. Fig. 3(c) also shows the verification of the optimized numerical results with Letchford and Sarkar [2].



(a) Effect of mesh size on accuracy of the numerical results



(b) Effect of number of mesh on accuracy of numerical results



(c) Verification between numerical and experimental data

Fig. 3. Numerical calibrations and verifications

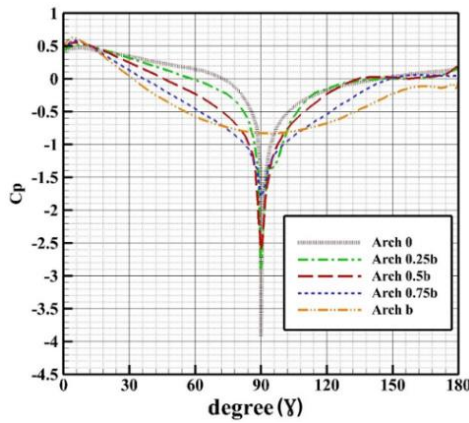


Fig. 4. The polygon for  $C_p$  at the central line parallel to the wind direction for different domes

Table 1. Min and max values of  $C_p$  on the central line parallel to the wind direction

The name of the dome	height - diameter proportion	minum pressure coefficient	Min $C_p - Arc0$	maximum pressure coefficient	Max $C_p - Arc0$	180 - $C_p(-)$ 180
Arch 0	0.5	-3.91	0	0.473	0	62.22%
Arch 0.25b	0.5	-2.89	26%	0.518	9.51%	52.41%
Arch 0.5b	0.5	-2.6	33.50%	0.558	17.97%	41.66%
Arch 0.75b	0.5	-1.79	54.22%	0.583	23.26%	37.22%
Arch b	0.5	-0.833	78.69%	0.631	33.40%	17.22%

#### 4. RESULTS AND DISCUSSIONS

Related results to the  $C_p$  observed at the central line parallel to the wind direction for the single-arched domes with a height-diameter proportion of 0.5 are presented in Fig. 4.

Moreover,  $C_p$  values obtained for the circles round the domes at different heights for the domes with height-diameter proportion of 0, 0.25b, 0.5b, 0.75b, and b are summarized in Table 1. For all Figures and counters, the direction of the wind is from left to right.

Results of the analysis showed that the max and min values of  $C_p$  are observed on the central line parallel to the wind direction for all five domes. A careful look at the graph reveals that the observed  $C_p$  increases from the angle of 0 up to the angle of 6 degrees, with the maximum pressure observed at the angle of 6 degrees, a finding that can be accounted for by the fact that at an angle of zero, the dome touches the ground which reduces the pressure exerted at this point. The comparison of the  $C_p$  values observed for the single arched domes shows that the increase in arch height is responsible for the maximal  $C_p$  for the front part of the dome facing the wind. It seems that the increment in the height causes the dome to be under suction at lower angles. Moreover,  $C_p$  equal to 0 is recorded at angles of 72, 57, 45, 37, and 31 degrees for domes with the arch height of 0, 0.25 b, 0.0.75b, and b in the windward region of the domes. The increment in the pressure is observed up to the top of the domes, where the minimum wind pressure is observed. Table 2 summarizes the data related to the percentage of the dome surface under wind pressure along the line parallel to the wind

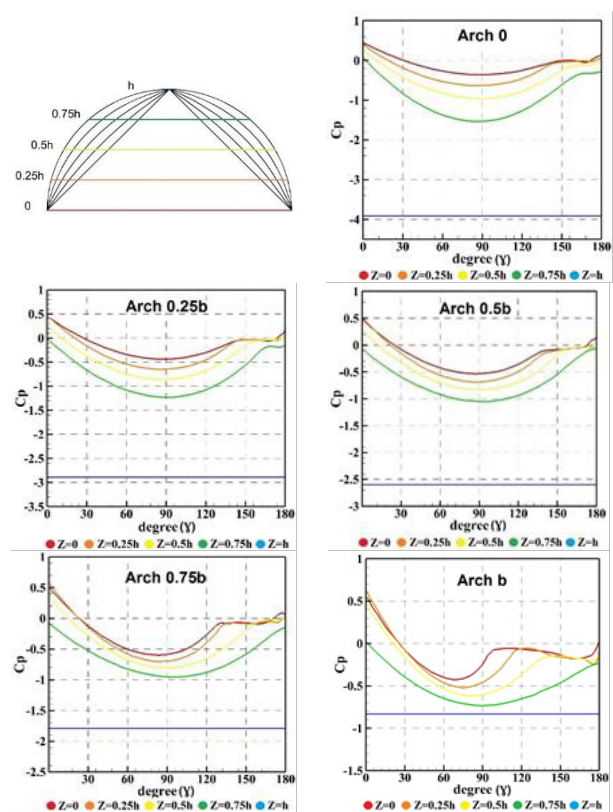


Fig. 5.  $C_p$  related to the height for different domes

Table 2. Absolute values of modified  $C_p$  relative to height

The name of the dome	0.25h - 0	0.25h - 0.5h	0.5h - 0.75h	h - 0.75h
Arch 0	0.61	0.93	1.52	3.91
Arch 0.25b	0.62	0.85	1.21	2.89
Arch 0.5b	0.69	0.82	1.08	2.60
Arch 0.75b	0.70	0.80	0.94	1.79
Arch b	0.63	0.63	0.74	0.83

direction for all the single arched domes.

For all the single arched domes, the minimum wind pressure rate experienced to be exerted in their top regions. In Table 2, the minimum  $C_p$  for the single arched domes, along with their deviations from the min  $C_p$  for the base dome is presented. The comparison of  $C_p$  along the circles surrounding the domes at heights of 0, 0.25h, 0.5h, 0.75h, h shows that the min  $C_p$  is observed for these heights along the line perpendicular to the wind direction. Moreover, as the height goes up, the point with min  $C_p$  moves toward the windward region of the dome.

$C_p$  of the dome at different heights, shown in the graph, is usually used for designing purposes.

#### 5. CONCLUSIONS

In the present study, the Effect of arch height on wind load of shape dome structure was investigated. Verification showed that the RANS-RNG turbulence model is an appropriate

model for the numerical simulation of domes. Results of this study showed that arch height plays an important role in the amount of lateral wind load on the domes. The max and min  $C_p$  occur on the central line parallel to the wind direction and at the front and top of the dome. By increasing the arch height, min and max  $C_p$  are decreased and increased, respectively. Also, under pressure surface is reduced with increasing arch height. Results of this study showed that the lowest amount of wind force is applied to the domes with the arch height of b,

0.25b, 0, 0.75b, and 0.5b, respectively.

## REFERENCES

- [1] T. Mahdi, Performance of Traditional Arches, Vaults and Domes in the 2003 BAM Earthquake, Asian Journal of Civil Engineering, 5(3-4) (2004).
- [2] C. Letchford, P. Sarkar, Mean and fluctuating wind loads on rough and smooth parabolic domes, Journal of wind engineering and industrial aerodynamics, 88(1) (2000) 101-117.

### HOW TO CITE THIS ARTICLE

S. Khosrowjerdi, H. Sarkardeh, *Effect of arch height on wind load in shape dome structure*, Amirkabir J. Civil Eng., 53(2) (2021) 145-148.

DOI: [10.22060/ceej.2020.16424.6220](https://doi.org/10.22060/ceej.2020.16424.6220)

